Title:

Lipid and Carbohydrate Modifications of α-Galactosylceramide Differently Influence Mouse andHuman Type I Natural Killer T cell activation

Author(s): Alysia Birkholz, Marek Nemčovič, Esther Dawen Yu, Enrico Girardi, Jing Wang,

Archana Khurana, Nora Pauwels, Elisa Farber, Sampada Chitale, Richard W. Franck,

Moriya Tsuji, Amy Howell, Serge Van Calenbergh, Mitchell Kronenberg, Dirk M.

Zajonc

Source: J. Biol. Chem. 2015, 290, 17206-17217

Lipid and Carbohydrate Modifications of α-Galactosylceramide Differently Influence Mouse and Human Type I Natural Killer T cell activation

Alysia Birkholz[1,2,3], Marek Nemčovič[1], Esther Dawen Yu[1], Enrico Girardi[1], Jing Wang[1], Archana Khurana[2], Nora Pauwels[4], Elisa Farber[7], Sampada Chitale[7], Richard W. Franck[5], Moriya Tsuji[6], Amy Howell[7], Serge Van Calenbergh[4], Mitchell Kronenberg[2,3], Dirk M. Zajonc[1,8]

[1] Division of Cell Biology, La Jolla Institute for Allergy & Immunology, La Jolla, California 92037, USA
[2] Division of Developmental Immunology, La Jolla Institute for Allergy & Immunology, La Jolla, CA 92037, USA
[3] Division of Biological Sciences, University of California, San Diego, La Jolla, California 92037, USA
[4] Laboratory for Medicinal Chemistry, Department of Pharmaceutics, Ghent University, 9000 Ghent, Belgium
[5] Department of Chemistry, Hunter College of CUNY, New York, NY 10021, USA
[6] Aaron Diamond AIDS Research Center, The Rockefeller University, New York, NY 10016, USA
[7] Department of Chemistry, University of Connecticut, Storrs, CT 06269, USA.
[8]Department of Internal Medicine, Faculty of Medicine and Health Sciences, Ghent University, 9000 Ghent, Belgium.

*Running Title: Effects of αGalCer structural modifications

To whom correspondence should be addressed: Dirk M. Zajonc, Division of Cell Biology, La Jolla Institute for Allergy & Immunology 9420 Athena Circle, La Jolla, CA, USA, Tel: (858) 752-6605; Fax: (858) 725-6985; E-mail: dzajonc@lji.org

Keywords: glycolipid structure; immunology; cytokine induction; protein crystallization

Background: Several synthetic glycosphingolipids have been tested to determine their capacity to activate Type I NKT cells.
Results: While the TCR binds with high affinity to all CD1d-presented glycolipids, only a few activate Type I NKT cells *in vivo*.
Conclusions: TCR binding affinity does not necessarily predict antigenicity *in vivo*.
Significance: The prediction of the therapeutic efficacy of Type I NKT cell antigens requires complementary assays.

ABSTRACT

The ability of different glycosphingolipids (GSLs) to activate Type I Natural Killer T cells (NKT cells) has been known for two decades. The possible therapeutic use of these GSLs has been studied in many ways, however studies in which the efficacy of promising GSLs is compared under identical conditions are missing. Here we compare five unique GSLs structurally derived from α-galactosylceramide (αGalCer). We employed biophysical and biological assays, as well as X-ray crystallography to study the impact of the chemical modifications of the antigen on Type I NKT cell activation. While all glycolipids are bound by the TCR of Type I NKT cells in real-time binding assays with high affinity, only a few activate Type I NKT cells in *in vivo* or *in vitro* experiments. The differences in biological responses are likely a result of different pharmacokinetic properties of each lipid, which carry modifications at different parts of the molecule. Our results indicate a need

to perform a variety of assays to ascertain the therapeutic potential of Type I NKT cell GSL activators.

Natural Killer T (NKT) cells are a unique population of T lymphocytes with the capacity to impact a wide array of functions of the immune system, ranging from protection against infections to responses to tumors and the regulation of autoimmunity (1,2). These cells accomplish this feat through their ability to secrete T helper type 1 (Th1) and T helper type 2 (Th2) cytokines, most notably IFN-γ and IL-4, respectively, and their ability to impact other white blood cells, such as natural killer (NK) cells, dendritic cells and B cells (3-5). NKT cells, specifically Type I NKT cells, have a semi-invariant T-cell antigen receptor (TCR) that has an evolutionarily conserved alpha chain, formed by a Vα14/Jα18 joining in mice and a homologous Vα24/Jα18 in humans (3). The TCR α chain, pairs with a less restricted β chain repertoire, to impart a specificity for glycosphingolipids (GSLs) presented by CD1d. CD1d is a member of the CD1 family of antigen presenting molecules (CD1a-e in humans, CD1d in mice) that is structurally similar to peptide presenting MHC class I antigen presenting molecules (6). The CD1d heavy chain is composed of three domains, α1, α2 and α3. While the α3 domain non-covalently associates with β2-microglobulin, the α1-α2 superdomain forms a central, hydrophobic antigen binding groove (7). This groove further segregates into two connected pockets called A′ and F′. Each pocket binds one chain of a dual alkyl chain lipid antigen. In the case of GSLs, the sphingoid base binds in the F′ pocket, while the A′ pocket binds the fatty acid. This lipid binding orientation allows the sugar head group to be exposed in the center for recognition by the Type I NKT cell TCR, with the α chain of the TCR providing the predominate binding energy (8,9). Many GSLs have been analyzed for the activation of Type I NKT cell TCRs, but the most commonly studied is α-galactosylceramide (αGalCer) (10,11). This prototypical glycolipid activates Type I NKT cells to secrete both IL-4 and IFN-γ *in vivo* within 90 minutes. Since this initial discovery, many glycolipids have been studied that sway the response of the immune system predominately towards either a Th1 or a Th2 response (12). One of the earliest Th1 skewing lipids studied to date is C-glycoside, in which the O-glycosidic linkage of αGalCer is replaced with a methylene group, known to stabilize this lipid (13). Although this lipid causes a pronounced Th1 response in mice, it is unable to activate human Type I NKT cells. The importance of Th1 skewing in a mammalian system is important for driving the system towards an inflammatory response essential for tumor clearance (14) and vaccine adjuvant activity (15). Thus Type I NKT cell lipids that stimulate IFN-γ have been studied in the context of possible therapeutic development. Although much work has been done to analyze these cytokine skewed responses, the exact mechanism of cytokine polarization is not completely elucidated. In this study, we selected 5 different lipids, previously demonstrated to activate Type I NKT cells, and tested their ability to activate human and mouse Type I NKT cells, side-by-side. We have further assessed their TCR binding affinities and crystallized the mouse ternary CD1d-GSL-TCR complexes to analyze the molecular interactions that ultimately lead to TCR triggering.

EXPERIMENTAL PROCEDURES

GSL synthesis- The GSLs used in this study have all been described previously: EF77 (16), GCK127 and 152 (17), NC-αGC (18), 7DW8-5 (19-23).

In vitro GSL presentation assays-

The GSL cell free presentation assay has been described previously (24). 96-well plates were coated with 1 μg of CD1d and were incubated overnight with various concentrations of GSLs. The CD1d molecules were then co-cultured with Type I NKT cell hybridomas overnight. The GSL cell based assay also has been described (25). Briefly, antigen presenting cells (APCs) (1×10^5 per well) were pulsed with 100 ng of the indicated lipid and were incubated overnight. The cells were then combined with 5×10^4 Vα14Vβ8.2 NKT cell hybridomas for 24 h. The DN3A4-1.2 (1.2)

Type I NKT hybridoma cell line has been described previously (26). TCR engagement was measured using a sandwich ELISA for IL-2 cytokines in the supernatant of hybridoma cultures.

Human Type I NKT cell assay- The isolation and expansion of human Vα24$^+$ NKT cell lines has been published previously (27). Human donor peripheral blood mononuclear cells (PBMCs, 1–1.5 $\times 10^6$/ml) were isolated and cultured in RPMI 1640 (Invitrogen) supplemented with 10% v/v) FBS and 1% (v/v) Pen-Strep-Glutamine (10,000 U penicillin, 10,000 µg streptomycin, 29.2 mg/ml L-glutamine; Invitrogen) and cultures were expanded by weekly re-stimulation with αGalCer-pulsed, irradiated PBMC and recombinant human IL-2. PBMCs (1×10^5 per well) were pulsed with GSLs and were seeded in 96 well plates and cultured in the presence of 5×10^4 Vα24$^+$ human NKT cells for 24 h. GM-CSF release was evaluated in a sandwich ELISA following the manufacturer's instructions (R&D Systems).

Mice- C57BL/6 were purchased from The Jackson Laboratory. All mice were housed in specific pathogen-free conditions and the experiments were approved by the Institutional Animal Care and Use Committee of the La Jolla Institute for Allergy & Immunology. Mice were injected with 1 µg of lipids intravenously and the sera of immunized mice were subjected to sandwich ELISAs to measure mouse IFN-γ levels.

Mouse and Human CD1d and TCR preparation- As reported previously (28), mouse CD1d-β2-microglobulin heterodimeric protein was expressed in a baculovirus expression system and human CD1d- β2-microglobulin was prepared similarly to the mouse protein. The TCR was prepared by refolding as previously reported (29).

CD1d loading- Each GSL was dissolved in DMSO at a concentration of 1 or 2 mg/mL. The individual GSLs were diluted in a vehicle solution (50 mM Tris-HCl pH 7.0, 4.8 mg/ml sucrose, 0.5 mg/ml sodium deoxycholate and 0.022% Tween 20) and were incubated at 80° C for at least 20 minutes. The GSLs were then combined with CD1d protein in an approximate 3:1 molar ratio of lipid to protein overnight in the presence of 50 mM Tris-HCl pH 7.0.

SPR kinetic analysis- Biotinylated CD1d was processed and purified and studies were conducted using a Biacore 3000 (GE Healthcare) as reported previously (29) and lipid loading was done as described above. Following overnight GSL loading, approximately 300 response units of CD1d-GSL complex were immobilized onto a streptavidin sensor chip surface by injecting the CD1d-GSL mixture at 5 µl/min using HBS (10 mM HEPES, 150 mM NaCl, 3.0 mM EDTA, pH 7.4) running buffer. A reference channel was bound with unloaded CD1d and increasing concentrations of refolded TCR were passed over at a flow rate of 30 µl/min. Kinetic association and dissociation curves were calculated using BIAevaluation software version 4.1.

Crystallization and structure determination- Following overnight GSL loading, the CD1d-GSL complexes were incubated with refolded TCR at room temperature for at least 30 minutes, followed by isolation of the complexes using Superdex S200 10/300 GL (GE Healthcare) equilibrated in buffer (50 mM Hepes pH 7.4, 150 mM NaCl). The isolated fractions containing the ternary complexes were concentrated and crystals were grown at 22.3°C by sitting drop vapor diffusion while mixing 0.5 µl protein solution with 0.5 µl precipitate. Precipitates were 0.2 M ammonium citrate dibasic pH 5.1 20% PEG 4000 for EF77, 17% polyethylene glycol, 8% tascimate pH 4 for 7DW8-5, 20% polyethylene glycol, 0.2 M ammonium citrate dibasic for NC-αGC, 17% polyethylene glycol, 0.2 M potassium acetate for GCK127 and 16% polyethylene glycol, 0.2 M ammonium citrate dibasic for GCK152. Single crystals were harvested and flash cooled in mother liquor containing 20% glycerol. Crystals were collected at the Stanford Synchrotron Radiation Lightsource and the Advanced Light Source and processed with the software Mosflm (30) or HKL2000 (31). The structures were solved by molecular replacement in CCP4 (Collaborative Computational Project, Number 4) (32). First, the coordinates for the CD1d protein of PDB

ID 2Q7Y were used, followed by the TCR coordinates of PDB ID 3QUZ. Models were rebuilt into σ_A-weighted $2Fo - Fc$ and $Fo - Fc$ difference electron density maps using COOT (33). The GSLs were built into $2Fo - Fc$ map and refined using REFMAC (34). Refmac geometric libraries for the glycolipids were obtained using the PRODRG server (35). Data collection and refinement statistics are summarized in Table 2.

RESULTS

Modifications of the αGalCer structure- We have compared the structure and antigenicity of αGalCer analogs modified in three different parts: the galactose headgroup, fatty acyl chain and the sphingoid base (Figure 1). In addition, GCK127 and GCK152 have their *O*-glycosidic linkages replaced with an *E*-alkene linker between the sugar and lipid moieties, reminiscent of C-glycoside (α-C-GalCer), while GCK152 also has a truncated fatty acid with a terminal phenyl group (C8-Ph) (17). Naphthylcarba-αGalCer (NC-αGC) has an aromatic 6"-OH galactose modification, similar to the previously crystalized naphthylurea (NU)-αGC. However, unlike NU-αGC where the naphthyl is linked via a urea group, NC-αGC has a carbamate linker, which provides more flexibility to the naphthyl moiety (18). The rationale of introducing this flexible linker was to assess whether the rigidity of the urea linker or the aromatic nature and size of the naphthyl group cause the reported structural change in the A′ roof of CD1d (36). EF77 is a plakoside A-like glycolipid, a GSL isolated from the marine sponge, *Plakortis simplex* (37), and is related to the previously crystallized SMC124 lipid (16). The sugar head group and *O*-glycosidic linkage are identical to αGalCer but the acyl chain has been modified to mimic plakoside A, with a cyclopropyl group and double bond between carbons 4 and 5 (16). Like EF77, 7DW8-5 also has a modification in the acyl group. The length of the chain has been shortened to 11 carbons and a parafluor-phenyl group has been added (C11-Ph-F) (19,20). The rational behind those different modifications is that changes in the lipid moiety would be expected to mainly influence the lipid interaction with CD1d, while changes in the galactose moiety and linkage can affect interaction with CD1d, the TCR and they could confer resistance to endoglycosidases upon injection into mice, and thus could increase the half-life in serum.

Real-time TCR binding kinetics- First, we determined the TCR interactions of these lipids presented by both mouse and human CD1d using Surface Plasmon Resonance (SPR) (Figure 2). As has been seen previously, the affinity of the mouse TCR to the GSL-CD1d complexes is higher (in the nM range) whereas the affinity of the human TCR for the GSL-CD1d complexes is weaker (in the μM range). According to the analysis using mouse CD1d and TCR (Figure 2A), the lipids cluster into a lower affinity and a higher affinity group. GCK127 (K_D=247 ± 86 nM) and GCK152 (K_D=197 ± 22 nM) show the lowest Vα14Vβ8.2 TCR affinity. This is similar to the affinity reported for the parent α-C-GalCer (K_D=247 nM, (36), but approximately 10-fold weaker than αGalCer, which in our hands ranges in affinity from 11 to 25 nM (29,38). Of note, the binding affinity is still high compared to mouse TCR affinities for MHC presented peptides, which most often are in the micromolar range (39,40). The higher affinity group is comprised of the NC-αGC (K_D=37.1 ± 14.10 nM), similar to NU-αGC (36), EF77 (44.7 ± 0.4 nM) and 7DW8-5 (94 ± 2.8 nM). The division into lower and higher affinity groups was not maintained in the SPR analysis using the human Vα24Vβ11 TCR and human CD1d (Figure 2B). GCK152 and EF77 were the weakest binders with K_D-values of 6.85 ± 2.6 μM and 3.4 ± 2.71 μM, respectively. The other lipids had similar affinity to αGalCer, which in our hands ranges from 1-3 μM. GCK127 (1.45 ± 0.05 μM) and NC-αGC (1.45 ± 0.35 μM) were very similar and 7DW8-5 resulted in the highest TCR affinity (1.13 ± 0.9 μM). We noted that in the mouse studies the off-rate for the Type I NKT cell TCR for both GCK127 and GCK152 (k_d =1.28 ± 0.0014 x 10^{-2} s^{-1} and 1.66 ± 0.0016 x10^{-2} s^{-1}, respectively) is 10x faster than the other ligands including αGalCer (k_d= 2.2 ± 0.52 x 10^{-3} s^{-1}) (data not shown) but similar to α-C-GalCer (36). Therefore, we assume that

the GCK glycolipids were not able to induce the closure of the roof over the CD1d F' pocket. As previously reported, some GSLs like αGalCer induce the formation of the F' roof closure prior to TCR docking, through orienting CD1d side chains at L84, V149, and L150 to an optimal conformation for engagement by the TCR CDR3α residue L99. The pre-formed F' roof closure has been correlated with a slower off-rate of the Type I NKT cell TCR (41). In the human SPR studies we noted that the off-rates for all the GSLs were similar, likely due to the inability of human CD1d to pre-form the closed F' roof, as the L84 of mouse CD1d is altered to F84 in human CD1d and a fully closed F' roof has not been observed in the hCD1d-αGalCer structure (42).

Crystal structures of the trimolecular complexes- In order to determine how each of these lipids is recognized by the TCR of Type I NKT cells, we crystallized each lipid in complex with mouse CD1d and the mouse Vα 14Vβ8.2 TCR. Crystallographic parameters are listed in Table 2. The overall structures of all complexes were consistent with the previously crystallized CD1d-glycolipid-TCR complexes, with the TCR docked offset over the F′ pocket of CD1d in a parallel orientation to the two α helices (Figure 3), notably different from the diagonal footprint generated in MHC-peptide-TCR complexes. All GSLs bind with the fatty acid chain in the A′ pocket of CD1d, he sphingoid base nestles inside the F′ pocket and the galactose moiety exposed at the CD1d binding groove portal for TCR recognition. Electron density for all of the lipids is well defined except for the acyl chain of 7DW8-5 (Figure 4). In this case, the electron density implies that the acyl chain can orient itself both clockwise and counterclockwise around cysteine 12 within the A' binding pocket. Thus, we have modeled both acyl chain orientations of 7DW8-5 with 50% occupancy (occurrence) (Figure 4F).

TCR-interactions- Previous studies established that the TCR of Type I NKT cells binds CD1d with a largely conserved binding footprint (43-46). Not surprisingly, the contact surfaces between CD1d and the TCR are very similar throughout the different ternary complexes (Table 2). All the TCR interactions with the antigen are formed with the conserved TCR α chain, while both TCR chains contact CD1d. TCR interactions with CD1d are dominated by the TCR α chain (818-870Å^2 total buried surface area, BSA), but there is substantial involvement of the TCR β chain (582-650Å^2 BSA) (Table 2). Contacts between TCRα and the ligand vary depending on the ligand modification, resulting in subtle differences in the presentation of the sugar to the TCR. Crystal structure analysis shows hydrogen bonding is maintained similar to αGalCer in the cases of 7DW8-5, GCK127 and EF77, with contacts between the galactose and residues N30, R95 and G96 of the Type I NKT TCR α chain (Figure 4). GCK152 shows the most deviation from this binding. It fails to maintain the hydrogen bonds between the 4" hydroxyl group and N30, and the 3" hydroxyl group and R95 of the TCR. Furthermore, it also fails to make a hydrogen bond between the 3' sphingoid base hydroxyl group and D80 of the CD1d molecule. These differences likely partially account for its reduced TCR affinity. NC-αGC loses the hydrogen bond between the 4" hydroxyl group of the sugar and N30 of the TCR (Figure 5C). It should be noted that due to the moderate resolution of the different complexes, a precise hydrogen-bond distance is not given and generally a cut-off of 3.5Å distance is applied. Similarly to the previously crystallized NU-αGC, the naphthyl anchor binds within a newly formed pocket in the A' roof of CD1d, slightly pulling the galactose away from the TCR. Although NC-αGC was predicted to be more flexible than NU-αGC, when the two structures are overlayed (Figure 5F), there are no discernable differences between them at the resolution of this study, suggesting that the size and nature of the aromatic modification, and not the flexibility of the linker region, drives the induced fit observed in CD1d. We noted that the total buried surface area between the TCRα and GSL was highest in the group of three ligands with the highest TCR affinity, NC-αGC, EF77 and 7DW8-5 (Table 2). However, considering NC-αGC, the number of H-bonds between TCR and antigen did not

always correlate with the affinity, suggesting that van der Waals interactions can contribute greatly to the TCR binding affinity and can compensate for the loss of individual hydrogen bond interactions (Figure 5).

Biological activity of the glycolipids- As all glycolipid antigens were bound by the TCR with moderate to high affinity, we investigated their activity *in vitro* and *in vivo*. Different biological assays for each of the glycolipids have been reported previously, EF77 (16), GCK127 and 152 (17), NC-αGC (18), 7DW8-5 (19-23), however, here we assess their potency side-by-side using the same assays. First, we performed a cell-based antigen presentation assay, in which a mouse B-cell lymphoma cell line (A20) stably expressing CD1d was pulsed with various lipids and their ability to activate the mouse Vα14Vβ8.2 NKT cell hybridoma cell line 1.2 was analyzed. TCR engagement and subsequent hybridoma activation was measured by IL-2 secretion. All the GSLs stimulated the hybridoma compared to the mock control, with 7DW8-5, EF77 and GCK152 giving the most potent response (Figure 6A).

The ultimate goal for the synthesis of novel GSLs is to develop a possible therapeutic agent for human use. To address whether these lipids could activate human Type I NKT cells, we used a model whereby antigen-presenting cells in the form of PBMCs and Type I NKT cells were isolated from normal human donor blood samples. Various concentrations of lipids were added to PBMCs and activation of human Type I NKT cells was measured by GM-CSF cytokine secretion in the supernatant (one representative graph is shown, Figure 6B). 7DW8-5, NC-αGC and EF77 are strong activators, capable of stimulating human Type I NKT cells in a dose-dependent manner. However, high concentrations of NC-αGC seemed to inhibit Type I NKT cell activation. In comparison, both alkene versions of the parental C-glycoside compound, GCK127 and GCK152, failed to activate human Type I NKT cells, even at high concentrations.

We further tested the lipids *in vivo* by i.v. injection of 1 μg of each lipid into mice. 24 h post injection, we analyzed serum IFN-γ cytokine levels using a sandwich ELISA. NC-αGC and EF77 were able to generate a pronounced, systemic IFN-γ burst at this timepoint (Figure 6C). To test whether the inability of the GCK compounds to show a strong response in any biological assay is due to unexpected degradation of the glycolipids during storage, we performed a cell free antigen presentation assay. Recombinant CD1d was coated in 96 well plates, incubated overnight with the indicated concentration of glycolipids and cultured with the Vα14Vβ8.2 NKT cell hybridoma 1.2. We expected that glycolipids that result in a strong TCR binding affinity should also induce robust T cell hybridoma activation, since TCR triggering and subsequent T cell activation is independent of T cell co-stimulation. As such, we expected a correlation between TCR binding strength and cytokine production. Both GCK127 and GCK152 induced a robust IL-2 secretion, demonstrating that both lipids were still fully intact throughout the course of this study (Figure 6D). The same pattern was observed using a different Type I NKT cell hybridoma (data not shown). GCK127 and GCK152 induced a lower IL-2 production, compared to 7DW8-5 and EF77, in correlating with their lower TCR affinity. However, surprisingly, NC-αGC, which had the highest TCR affinity, gave the lowest response.

In summary, we measured the formation of the trimolecular complex of CD1d, GSL antigen and the TCR by SPR and analyzed the nature of the molecular interactions by X-ray crystallography. This analysis provided insights into the ways these antigens can be bound and recognized. Differences in TCR affinity and binding kinetics were not highly predictive even of the ability of the compounds to stimulate Type I NKT cell hybridomas in a cell-free antigen presentation assay. They were less predictive of the ability to stimulate Type I NKT cell cytokine responses *in vivo*. Therefore, other properties, including solubility, interactions with lipid binding proteins, uptake by different cell types and chemical stability of each lipid appear to affect stimulation of Type I NKT cells. While NC-αGC is not able to activate Type I NKT cells when pulsed into A20 cells,

it strongly activates human Type I NKT cells using pulsed PBMCs and murine Type I NKT cells when injected intravenously into mice. In contrast, 7DW8-5 potently activates human Type I NKT cells and murine Type I NKT cell hybridomas using pulsed A20 cells but not when injected intravenously. EF77 was the only lipid that gave strong responses in all three assays, while the GCK series failed to give a robust response *in vivo* or in cell based assays, even though the TCR binding kinetics were among the strongest for human Type I NKT cells (Figure 2).

DISCUSSION

Many Type I NKT cell activating GSLs have been assessed to determine how they stimulate the human and mouse immune systems (12). Analysis of GSLs reported to be Th1 skewing clearly indicate that a variety of parameters are in play that will determine the *in vivo* immune response in mice and humans, and potency cannot be predicted by a purely biochemical approach or by any one type of assay. As mouse and human Type I NKT cells have different fine specificities for CD1d presented antigens, structural studies of the human complexes are important to dissect the underlying structural differences (47). However, we were unsuccessful to obtain the required resolution for robust structure determination using the human molecules. Instead, biochemical approaches can yield important insights into the mechanism that governs the binding reaction and they can contribute to the design of even more effective stimulators of Type I NKT cells. For example, it is interesting to note that although the linker of NU-αGC has been altered in the NC-αGC lipid, allowing for more flexibility of the naphthyl group, the two crystal structures show no obvious differences and the overlay indicates the conserved binding orientation of the Type I NKT cell TCR trumps flexibility in these models. NC-αGC is a very strong antigen *in vivo* in mice and *in vitro* for humans. Although it lacks activity in the *in vitro* cell presentation assay, we hypothesize that this may reflect reduced *in vitro* CD1d loading efficiency, due to the aromatic naphtyl moiety, which reduces water solubility, or possibly the absence of a crucial lipid binding or transport protein derived from the APCs, subsequently leading to less stimulatory CD1d molecules and thus less T cell activation. Conversely, EF77, the plakoside A GSL, demonstrates potent activity in all assays. 7DW8-5 activates mouse and human Type I NKT cells *in vitro* in the presence of APCs, and the ability of 7DW8-5 to activate human Type I NKT cells correlates with previously reported data that this GSL is able to serve as a vaccine adjuvant in primate models. Although this GSL does not cause robust IFN-γ cytokine secretion in our mouse *in vivo* system, this could be due to the fact that this lipid may biodistribute differently than other GSLs after i.v. injection, perhaps a different route is used in primates. It has been noted that mouse intramuscular injection of this lipid causes it to localize to local lymph nodes whereas αGalCer seems to go systemic (Moriya Tsuji, personal communication). The EF77 crystal structure showed similar features to its sister ligand SMC124. Both are related to plakoside A, but the EF77 ceramide has an αGalCer-like sphingosine and the plakoside A alkyl chain. The plakoside A acyl chain, with its cyclopropyl group, binds in the hydrophobic A' pocket of CD1d. SMC124 has the opposite configuration, with an αGalCer acyl chain and the plakoside A sphingoid base, which also has a cyclopropyl group, buried in the F' pocket (16). Similar to EF77, the acyl chain modified 7DW8-5 ligand shows the phenyl ring localizing to the A' groove, however, this GSL proved more difficult to model. Our crystal structure shows a duel binding motif of the acyl chain in the A' pocket indicating that the fatty acid chain may orient both clockwise and counterclockwise around C12, possibly altering its interaction with CD1d, rather than the TCR.

The GCK127 and GCK152 have the weakest affinity in the mouse SPR studies, with rapid off-rates, which may be in part due to the inability of the CD1d F' roof to pre-form prior to TCR engagement (48). This F' roof formation likely occurs upon binding of the other GSLs used in this study, accounting

for the 10-fold difference in dissociation rates in the mouse SPR studies. Because this pre-formation does not occur in human CD1d, we do not see a disparity in the dissociation rates of the human Type I NKT cell TCR. The GCK152 GSL also seems to fail to form some of the hydrogen bonds seen between αGalCer and CD1d and TCR, also accounting for a faster off-rate of the TCR. Although the human TCR affinities would predict a human Type I NKT cell response, GCK127 and GCK152 do not strongly activate the human cell lines in our hands similar to what was observed for the related α-C-GalCer. It is perhaps this alteration from an *O*-glycoside bond to a carbon linkage that slightly alters the binding of the glycolipid within CD1d. A rotation of the 3'-OH of the sphingoid base followed by concomitant loss of a hydrogen bond with Asp80 of CD1d has been observed in two separate crystal structures (36,49). Nonetheless, lipids of this nature do not appear to exhibit the same therapeutic potential than the other lipids in our assays. The buried surface area contacts between the TCRα loop and CD1d may shed some light on the variation in the biological and biochemical parameters. In conclusion, these different GSLs have the capacity to form interactions between CD1d and Type I NKT cells, but have various responses in the mouse and human studies, indicating a lack of one-to-one correlation.

Recent studies suggested that kinetic data obtained from TCR and peptide-MHC molecules in solution (e.g. by SPR), do not always correlate with T cell signaling outcome (50). Instead, measuring the interaction in 2D, where both MHC and TCR are each presented on a cell is a better predictor of the potency of an antigen. In the 2D system, a pulling force can be applied to mimic naturally occurring forces that occur when cells are in contact. Under those conditions, the TCR dissociation is 3-4 orders of magnitude increase compared to measurements carried out in solution (50,51). Applying these forces to the CD1d system would allow us to assess the role of the CD1d-lipid interaction in modulating the overall stability of the ternary complex, as interactions among all three molecules (antigen-CD1d, antigen-TCR, and CD1d-TCR) are likely important in the 2D system. When performing SPR studies, the stability of the CD1d-lipid complex does not affect TCR affinity, likely because no pulling forces are applied. Future studies could include the study of the 2D interaction using pulling force, while systematically changing the terminal lipid backbone, to alter its interaction with CD1d (50). Those assays would shed light on the contribution of the CD1d-lipid interaction in T cell triggering through modulating the stability and duration of their interaction. In addition, future studies that can accurately measure the pharmacokinetic properties of the GSLs, binding affinities for the GSL (see above) and CD1d molecules and biodistribution of different GSLs would be particularly interesting to address this outstanding issue.

REFERENCES

1. Robertson, F. C., Berzofsky, J. A., and Terabe, M. (2014) NKT cell networks in the regulation of tumor immunity. *Front. Immunol.* **5**, 543
2. Roozbeh, M., Mohammadpour, H., Azizi, G., Ghobadzadeh, S., and Mirshafiey, A. (2014) The potential role of iNKT cells in experimental allergic encephalitis and multiple sclerosis. *Immunopharmacol Immunotoxicol* **36**, 105–113
3. Bendelac, A., Savage, P. B., and Teyton, L. (2007) The Biology of NKT Cells. *Annu. Rev. Immunol.* **25**, 297–336
4. Brennan, P. J., Brigl, M., and Brenner, M. B. (2013) Invariant natural killer T cells: an innate activation scheme linked to diverse effector functions. *Nature Reviews Immunology* **13**, 101–117
5. Yu, K. O. A., and Porcelli, S. A. (2005) The diverse functions of CD1d-restricted NKT cells and their potential for immunotherapy. *Immunol. Lett.* **100**, 42–55
6. Calabi, F., and Milstein, C. (1986) A novel family of human major histocompatibility complex-related genes not mapping to chromosome 6. *Nature* **323**, 540–543
7. Zajonc, D. M., and Wilson, I. A. (2007) Architecture of CD1 Proteins. *T Cell Activation by CD1 and Lipid Antigens* **314**, 27–50
8. Borg, N. A., Wun, K. S., Kjer-Nielsen, L., Wilce, M. C. J., Pellicci, D. G., Koh, R., Besra, G. S., Bharadwaj, M., Godfrey, D. I., McCluskey, J., and Rossjohn, J. (2007) CD1d-lipid-antigen recognition by the semi-invariant NKT T-cell receptor. *Nature* **448**, 44–49
9. Pellicci, D. G., Patel, O., Kjer-Nielsen, L., Pang, S. S., Sullivan, L. C., Kyparissoudis, K., Brooks, A. G., Reid, H. H., Gras, S., Lucet, I. S., Koh, R., Smyth, M. J., Mallevaey, T., Matsuda, J. L., Gapin, L., McCluskey, J., Godfrey, D. I., and Rossjohn, J. (2009) Differential Recognition of Cd1d-a-Galactosyl Ceramide by the vb8.2 and Vb7 Semi-Invariant Nkt T Cell Receptors. *Immunity* **31**, 47–59
10. Morita, M., Motoki, K., Akimoto, K., Natori, T., Sakai, T., Sawa, E., Yamaji, K., Koezuka, Y., Kobayashi, E., and Fukushima, H. (1995) Structure-activity relationship of alpha-galactosylceramides against B16-bearing mice. *J. Med. Chem.* **38**, 2176–2187
11. Banchet-Cadeddu, A., Hénon, E., Dauchez, M., Renault, J.-H., Monneaux, F., and Haudrechy, A. (2011) The stimulating adventure of KRN 7000. *Org. Biomol. Chem.* **9**, 3080–3104
12. Anderson, B., Teyton, L., Bendelac, A., and Savage, P. (2013) Stimulation of Natural Killer T Cells by Glycolipids. *Molecules* **18**, 15662–15688
13. Schmieg, J., Yang, G., Franck, R. W., and Tsuji, M. (2003) Superior Protection against Malaria and Melanoma Metastases by a C-glycoside Analogue of the Natural Killer T Cell Ligand -Galactosylceramide. *Journal of Experimental Medicine* **198**, 1631–1641
14. Kakuta, S., Tagawa, Y.-I., Shibata, S., Nanno, M., and Iwakura, Y. (2002) Inhibition of B16 melanoma experimental metastasis by interferon-gamma through direct inhibition of cell proliferation and activation of antitumour host mechanisms. *Immunology* **105**, 92–100
15. Petrovsky, N., and Aguilar, J. C. (2004) Vaccine adjuvants: current state and future trends. *Immunol. Cell Biol.* **82**, 488–496
16. Tyznik, A. J., Farber, E., Girardi, E., Birkholz, A., Li, Y., Chitale, S., So, R., Arora, P., Khurana, A., Wang, J., Porcelli, S. A., Zajonc, D. M., Kronenberg, M., and Howell, A. R. (2011) Glycolipids that Elicit IFN-γ-Biased Responses from Natural Killer T Cells. *Chem. Biol.* **18**, 1620–1630
17. Li, X., Shiratsuchi, T., Chen, G., Dellabona, P., Casorati, G., Franck, R. W., and Tsuji,

M. (2009) Invariant TCR rather than CD1d shapes the preferential activities of C-glycoside analogues against human versus murine invariant NKT cells. *J. Immunol.* **183**, 4415–4421

18. Aspeslagh, S., Nemčovič, M., Pauwels, N., Venken, K., Wang, J., Van Calenbergh, S., Zajonc, D. M., and Elewaut, D. (2013) Enhanced TCR footprint by a novel glycolipid increases NKT-dependent tumor protection. *J. Immunol.* **191**, 2916–2925
19. Li, X., Fujio, M., Imamura, M., Wu, D., Vasan, S., Wong, C.-H., Ho, D. D., and Tsuji, M. (2010) Design of a potent CD1d-binding NKT cell ligand as a vaccine adjuvant. *Proc. Natl. Acad. Sci. U.S.A.* **107**, 13010–13015
20. Padte, N. N., Li, X., Tsuji, M., and Vasan, S. (2011) Clinical development of a novel CD1d-binding NKT cell ligand as a vaccine adjuvant. *Clinical Immunology* **140**, 142–151
21. Padte, N. N., Boente-Carrera, M., Andrews, C. D., McManus, J., Grasperge, B. F., Gettie, A., Coelho-dos-Reis, J. G., Li, X., Wu, D., Bruder, J. T., Sedegah, M., Patterson, N., Richie, T. L., Wong, C.-H., Ho, D. D., Vasan, S., and Tsuji, M. (2013) A Glycolipid Adjuvant, 7DW8-5, Enhances CD8+ T Cell Responses Induced by an Adenovirus-Vectored Malaria Vaccine in Non-Human Primates. *PLoS ONE* **8**, e78407
22. Venkataswamy, M. M., Ng, T. W., Kharkwal, S. S., Carreño, L. J., Johnson, A. J., Kunnath-Velayudhan, S., Liu, Z., Bittman, R., Jervis, P. J., Cox, L. R., Besra, G. S., Wen, X., Yuan, W., Tsuji, M., Li, X., Ho, D. D., Chan, J., Lee, S., Frothingham, R., Haynes, B. F., Panas, M. W., Gillard, G. O., Sixsmith, J. D., Korioth-Schmitz, B., Schmitz, J. E., Larsen, M. H., Jacobs, W. R., and Porcelli, S. A. (2014) Improving Mycobacterium bovis bacillus Calmette-Guèrin as a vaccine delivery vector for viral antigens by incorporation of glycolipid activators of NKT cells. *PLoS ONE* **9**, e108383
23. Xu, X., Hegazy, W. A. H., Guo, L., Gao, X., Courtney, A. N., Kurbanov, S., Liu, D., Tian, G., Manuel, E. R., Diamond, D. J., Hensel, M., and Metelitsa, L. S. (2014) Effective cancer vaccine platform based on attenuated salmonella and a type III secretion system. *Cancer Res.* **74**, 6260–6270
24. Naidenko, O. V., Maher, J. K., Ernst, W. A., Sakai, T., Modlin, R. L., and Kronenberg, M. (1999) Binding and antigen presentation of ceramide-containing glycolipids by soluble mouse and human CD1d molecules. *Journal of Experimental Medicine* **190**, 1069–1080
25. Lawton, A. P., Prigozy, T. I., Brossay, L., Pei, B., Khurana, A., Martin, D., Zhu, T., Späte, K., Ozga, M., Höning, S., Bakke, O., and Kronenberg, M. (2005) The mouse CD1d cytoplasmic tail mediates CD1d trafficking and antigen presentation by adaptor protein 3-dependent and -independent mechanisms. *The Journal of Immunology* **174**, 3179–3186
26. Brossay, L., Tangri, S., Bix, M., Cardell, S., Locksley, R., and Kronenberg, M. (1998) Mouse CD1-autoreactive T cells have diverse patterns of reactivity to CD1+ targets. *The Journal of Immunology* **160**, 3681–3688
27. Rogers, P. R., Matsumoto, A., Naidenko, O., Kronenberg, M., Mikayama, T., and Kato, S. (2004) Expansion of human Valpha24+ NKT cells by repeated stimulation with KRN7000. *Journal of Immunological Methods* **285**, 197–214
28. Zajonc, D. M., Maricic, I., Wu, D., Halder, R., Roy, K., Wong, C.-H., Kumar, V., and Wilson, I. A. (2005) Structural basis for CD1d presentation of a sulfatide derived from myelin and its implications for autoimmunity. *Journal of Experimental Medicine* **202**, 1517–1526
29. Wang, J., Li, Y., Kinjo, Y., Mac, T. T., Gibson, D., Painter, G. F., Kronenberg, M., and Zajonc, D. M. (2010) Lipid binding orientation within CD1d affects recognition of Borrelia burgorferi antigens by NKT cells. *Proceedings of the National Academy of Sciences* **107**, 1535–1540

30. Leslie, A. G. W. (2006) The integration of macromolecular diffraction data. *Acta Crystallogr. D Biol. Crystallogr.* **62**, 48–57
31. Otwinowski, Z., Minor, W., and W, C. C., Jr (1997) Processing of X-ray diffraction data collected in oscillation mode. **276**, 307–326
32. Winn, M. D., Ballard, C. C., Cowtan, K. D., Dodson, E. J., Emsley, P., Evans, P. R., Keegan, R. M., Krissinel, E. B., Leslie, A. G. W., McCoy, A., McNicholas, S. J., Murshudov, G. N., Pannu, N. S., Potterton, E. A., Powell, H. R., Read, R. J., Vagin, A., and Wilson, K. S. (2011) Overview of the CCP4 suite and current developments. *Acta Crystallogr. D Biol. Crystallogr.* **67**, 235–242
33. Emsley, P., Lohkamp, B., Scott, W. G., and Cowtan, K. (2010) Features and development of Coot. *Acta Crystallogr. D Biol. Crystallogr.* **66**, 486–501
34. Vagin, A. A., Steiner, R. A., Lebedev, A. A., Potterton, L., McNicholas, S., Long, F., and Murshudov, G. N. (2004) REFMAC5 dictionary: organization of prior chemical knowledge and guidelines for its use. *Acta Crystallogr. D Biol. Crystallogr.* **60**, 2184–2195
35. Schüttelkopf, A. W., and van Aalten, D. M. F. (2004) PRODRG: a tool for high-throughput crystallography of protein-ligand complexes. *Acta Crystallogr. D Biol. Crystallogr.* **60**, 1355–1363
36. Aspeslagh, S., Li, Y., Yu, E. D., Pauwels, N., Trappeniers, M., Girardi, E., Decruy, T., Van Beneden, K., Venken, K., Drennan, M., Leybaert, L., Wang, J., Franck, R. W., Van Calenbergh, S., Zajonc, D. M., and Elewaut, D. (2011) Galactose-modified iNKT cell agonists stabilized by an induced fit of CD1d prevent tumour metastasis. *EMBO J.* **30**, 2294–2305
37. Costantino, V., Fattorusso, E., Mangoni, A., Di Rosa, M., and Ianaro, A. (1997) Glycolipids from Sponges. 6. 1Plakoside A and B, Two Unique Prenylated Glycosphingolipids with Immunosuppressive Activity from the Marine Sponge Plakortis simplex. *J. Am. Chem. Soc.* **119**, 12465–12470
38. Aspeslagh, S., Nemcovic, M., Pauwels, N., Venken, K., Wang, J., Van Calenbergh, S., Zajonc, D. M., and Elewaut, D. (2013) Enhanced TCR Footprint by a Novel Glycolipid Increases NKT-dependent Tumor Protection. *J. Immunol.* **191**, 2916–2925
39. Rudolph, M. G., Stanfield, R. L., and Wilson, I. A. (2006) How TCRs bind MHCs, peptides, and coreceptors. *Annu. Rev. Immunol.* **24**, 419–466
40. Rossjohn J, Gras S, Miles JJ, Turner SJ, Godfrey DI, McCluskey J. T cell antigen receptor recognition of antigen-presenting molecules. Annu Rev Immunol. 2015;33:169-200. doi: 10.1146/annurev-immunol-032414-112334. PubMed PMID: 25493333.
41. Li, Y., Girardi, E., Wang, J., Yu, E. D., Painter, G. F., Kronenberg, M., and Zajonc, D. M. (2010) The Vα14 invariant natural killer T cell TCR forces microbial glycolipids and CD1d into a conserved binding mode. *J Exp Med* **207**, 2383–2393
42. Koch, M., Stronge, V. S., Shepherd, D., Gadola, S. D., Mathew, B., Ritter, G., Fersht, A. R., Besra, G. S., Schmidt, R. R., Jones, E. Y., and Cerundolo, V. (2005) The crystal structure of human CD1d with and without α-galactosylceramide. *Nat. Immunol.* **6**, 819–826
43. Mallevaey, T., Clarke, A. J., Scott-Browne, J. P., Young, M. H., Roisman, L. C., Pellicci, D. G., Patel, O., Vivian, J. P., Matsuda, J. L., McCluskey, J., Godfrey, D. I., Marrack, P., Rossjohn, J., and Gapin, L. (2011) A molecular basis for NKT cell recognition of CD1d-self-antigen. *Immunity* **34**, 315–326
44. Wun, K. S., Cameron, G., Patel, O., Pang, S. S., Pellicci, D. G., Sullivan, L. C., Keshipeddy, S., Young, M. H., Uldrich, A. P., Thakur, M. S., Richardson, S. K., Howell, A. R., Illarionov, P. A., Brooks, A. G., Besra, G. S., McCluskey, J., Gapin, L., Porcelli, S. A., Godfrey, D. I., and Rossjohn, J. (2011) A Molecular Basis for the Exquisite CD1d-Restricted Antigen Specificity and Functional Responses of Natural

Killer T Cells. *Immunity* **34**, 327–339
45. Girardi, E., and Zajonc, D. M. (2012) Molecular basis of lipid antigen presentation by CD1d and recognition by natural killer T cells. *Immunol Rev* **250**, 167–179
46. Rossjohn J, Pellicci DG, Patel O, Gapin L, Godfrey DI. Recognition of CD1d-restricted antigens by natural killer T cells. Nat Rev Immunol. 2012;12(12):845-57. doi: 10.1038/nri3328. PubMed PMID: 23154222; PubMed Central PMCID: PMC3740582.
47. Wun KS, Ross F, Patel O, Besra GS, Porcelli SA, Richardson SK, et al. Human and mouse type I natural killer T cell antigen receptors exhibit different fine specificities for CD1d-antigen complex. J Biol Chem. 2012;287(46):39139-48. doi: 10.1074/jbc.M112.412320. PubMed PMID: 22995911; PubMed Central PMCID: PMC3493954.
48. Joyce, S., Girardi, E., and Zajonc, D. M. (2011) NKT Cell Ligand Recognition Logic: Molecular Basis for a Synaptic Duet and Transmission of Inflammatory Effectors. *The Journal of Immunology* **187**, 1081–1089
49. Patel, O., Cameron, G., Pellicci, D. G., Liu, Z., Byun, H. S., Beddoe, T., McCluskey, J., Franck, R. W., Castaño, A. R., Harrak, Y., Llebaria, A., Bittman, R., Porcelli, S. A., Godfrey, D. I., and Rossjohn, J. (2011) NKT TCR Recognition of CD1d-α-C-Galactosylceramide. *The Journal of Immunology* **187**, 4705–4713
50. Huang J, Zarnitsyna VI, Liu B, Edwards LJ, Jiang N, Evavold BD, et al. The kinetics of two-dimensional TCR and pMHC interactions determine T-cell responsiveness. Nature. 2010;464(7290):932-6. doi: 10.1038/nature08944. PubMed PMID: 20357766; PubMed Central PMCID: PMC2925443.
51. Liu B, Chen W, Evavold BD, Zhu C. Accumulation of dynamic catch bonds between TCR and agonist peptide-MHC triggers T cell signaling. Cell. 2014;157(2):357-68. doi: 10.1016/j.cell.2014.02.053. PubMed PMID: 24725404; PubMed Central PMCID: PMC4123688.

Acknowledgements: The authors would like to thank the Stanford Synchrotron Radiation Lightsource and the Advanced Light Source for access to remote data collection. Use of the Stanford Synchrotron Radiation Lightsource, SLAC National Accelerator Laboratory, is supported by the U.S. Department of Energy, Office of Science, Office of Basic Energy Sciences under Contract No. DE-AC02-76SF00515. The SSRL Structural Molecular Biology Program is supported by the DOE Office of Biological and Environmental Research, and by the National Institutes of Health, National Institute of General Medical Sciences (including P41GM103393). The contents of this publication are solely the responsibility of the authors and do not necessarily represent the official views of NIGMS or NIH. The Advanced Light Source is supported by the Director, Office of Science, Office of Basic Energy Sciences, of the U.S. Department of Energy under Contract No. DE-AC02-05CH11231.

FOOTNOTES

*****This work was supported by NIH grants RO1 AI074952, R21 AI107318 (D.M.Z.), NIH RO1 grants AI45053, AI71922 (M.K.), NIH RO1 grant GM087136 (A.H.) and NIH RO1 AI070258 (M.T.). S.V.C. received support from the Belgian Stichting tegen Kanker, the FWO Flanders, and the research council of Ghent University. M.N. received support from the Slovak American Foundation.

[1,8] To whom correspondence should be addressed: Dirk M. Zajonc, Division of Cell Biology, La Jolla Institute for Allergy & Immunology 9420 Athena Circle, La Jolla, CA, USA, Tel: (858) 752-6605; Fax: (858) 725-6985; E-mail: dzajonc@lji.org

Current addresses of authors:
Enrico Girardi: CeMM, Research Center for Molecular Medicine of the Austrian Academy of Sciences, A-1090 Vienna, Austria
Esther Yu: Duke-NUS Graduate Medical School Singapore, 8 College Road, Singapore 169857
Marek Nemčovič: Institute of Chemistry, Slovak Academy of Sciences, Bratislava, Slovakia
Nora Pauwels: Wipa Chemicals International N.V., Evergem, Belgium

Abbreviations:
Å: angstrom
αGalCer: α-galactosylceramide
APC: antigen presenting cell
GSL: glycosphingolipid
MHC: major histocompatibility complex
NK: natural killer
NKT: natural killer T-cell
iGB3: isoglobotrihexosylceramide
SPR: surface plasmon resonance
TCR: T cell receptor
Th1: T helper type 1
Th2: T helper type 2

FIGURE LEGENDS:

FIGURE 1. Chemical structures of glycosphingolipids. In green, the carbohydrate galactose sugar moiety, in red the fatty acid chain and in blue, the sphingoid base of αGalCer. In yellow, structural modifications of each GSL compared to the αGalCer template structure.

FIGURE 2. Real-time TCR binding kinetics. Binding of refolded mouse Vα14Vβ8.2 TCR (A) or human Vα24Vβ11 TCR (B) to the indicated glycolipids presented by mouse and human CD1d, respectively. One representative sensorgram is depicted at the bottom showing the binding response of increasing concentrations of TCR (colored curves) and the calculated fit (black curves).

FIGURE 3. Ternary crystal structures of mouse CD1d-GSL- Vα14Vβ8.2 NKT cell TCR complexes. A. GCK152 B.GCK127 C. NC-αGC D. 7DW8-5 E. EF77. CD1d in grey, β_2M in blue. TCRα chain in cyan and TCRβ chain in orange.

FIGURE 4. Electron Density of GSLs shown with CD1d. Note: α2 helix removed for clarity A. NC-αGC B. EF77 C. 7DW8-5 D. GCK152 E. GCK127 F. dual binding motif for acyl chain of 7DW8-5. $2F_oF_c$ electron density is drawn as a blue mesh around the glycolipid (colored sticks) and contoured at 1σ. CD1d in grey

FIGURE 5. Mouse Vα14Vβ8.2 NKT cell TCR hydrogen bond interactions with CD1d and GSLs A. GCK127 B. GCK152 C.NC-αGC D. 7DW8-5 E. EF77 F. Overlay of NC-αGC (cyan) with NU-αGC (purple) ribbon crystal structures. Hydrogen bonds between TCRα (in cyan) and the various glycolipids (colored sticks) are indicated by blue dashed lines. Individual OH groups of the galactose sugar that participate in hydrogen bonding are labeled with position. CD1d α1-helix as a reference shown in grey.

FIGURE 6. Biological Assays with GSLs A. Cell based assay in which an A20 B cell lymphoma cell line transfected with CD1d was pulsed with 100 ng of the indicated GSL and co-cultured with a Vα14Vβ8.2 NKT cell hybridoma (1.2). TCR engagement measured after 24 hours through IL-2 production in serum measured with a sandwich ELISA. Data represents samples in triplicate and is representative of three independent experiments. B. Human Type I NKT cells were activated by human PBMCs pulsed with the indicated glycolipid concentrations 24 h. Cytokine levels for human GM-CSF were measured in the supernatant using a sandwich ELISA assay. Representative data from one of two experiments performed in triplicate wells using multiple human cell lines are shown. C. C57Bl/6 mice were injected with 1 μg of the indicated GSL, and sera were analyzed at 24 hours. Serum samples were measured for IFN-γ cytokine levels by ELISA. Data are representative of 2 independent experiments of 3 mice per group. Error bars represent ± SEM. D. Cell free antigen presentation assay. 96 well plates were coated with recombinant CD1d and incubated overnight with indicated concentration of glycolipids. After the initial incubation, Vα14Vβ8.2 NKT cell hybridoma 1.2 was added overnight. Serum IL-2 was measured using a sandwich ELISA. Representative data from 1 of 2 different hybridoma lines are shown.

TABLES

TABLE 1. Refinement statistics for the CD1d-GSL-TCR complexes

Data collection statistics	**CD1d-GCK127-TCR**	**CD1d-GCK152-TCR**	**CD1d-NC-αGC-TCR**	**CD1d-EF77-TCR**	**CD1d-7DW8-5-TCR**
PDB ID	4Y4F	4Y4H	4Y16	4Y4K	4Y2D
Space group	$P2_1$	$P2_1$	$C222_1$	$C222_1$	$P2_1$
Cell dimension					
a, b, c, (Å)	78.6, 149.7, 101.4	79.4, 150.4, 102.5	79.6, 191.9, 151.9	79.1, 191.4, 151.3	79.4, 150.3, 100.8
α, β, γ (°)	90, 96.5,90	90, 96.4, 90	90, 90, 90	90, 90, 90	90, 96.2, 90
Resolution range (Å) [outer shell]	40-3.2 [3.31-3.2]	40-3.1 [3.15-3.1]	66.21-2.60 [2.71-2.60]	95.7-2.9 [3.06-2.9]	500-3.05 [3.12-3.05]
No. reflections	38,286	42,694	34,681	25,092	44,418
R_{merge} (%)	13 [63.9]	11.3 [59.9]	10.3 [47.8]	17.2 [59.4]	9.3 [53.6]
R_{pim} (%)	n/a	n/a	7.0 [32.6]	11.1 [38.4]	n/a
Multiplicity	3.3 [3.3]	3.8 [4.0]	2.9 [2.9]	3.2 [3.4]	3.0 [3.0]
Average I/sI	13.7 [2.1]	21.5 [2.7]	6.8 [2.3]	5.9 [2.2]	13.2 [2.0]
Completeness (%)	98.2 [91.1]	99.4 [100]	96.2 [95.7]	97.4 [99.1]	99.3 [99.8]
Refinement statistics					
No. atoms	12,599	12,469	6,532	6,305	11,943
Protein	12,389	12,247	6,333	6,183	11,627
Ligand	126	96	73	56	208
Carbohydrate	84	126	80	66	108
Water	0	0	46	0	0
R/R_{free} (%)	21.8/25.7	24.2/28.3	21.1/24.4	21.9/26.5	21.7/25.7
Ramachandran plot (%)					
Favored	96.91	95.52	96.36	96.11	95.93
Allowed	99.75	99.68	100	99.75	99.87
R.m.s. deviations					
Bonds (Å)	0.006	0.01	0.01	0.005	0.005

Angles (°)	0.879	1.226	1.248	1.076	0.994
B-factors (Å^2)					
Protein	89.25	75.42	41.75	37.58	75.66
Ligand	67.87	58.88	33.77	28	50.79
Carbohydrate	83.86	87.85	54.56	44.54	96.54

TABLE 2. Total Buried surface areas between mouse TCR-CD1d and TCRα-glycolipid (in Å^3)

	CD1d-ligand-TCR complex				
Contact surfaces	GCK127	GCK152	NC-αGC	EF77	7DW8-5
TCRα-ligand	298	290	298	303	241
TCRα-CD1d	844	818	867	854	870
TCRβ-CD1d	610	647	633	637	582

FIGURES

Figure 1

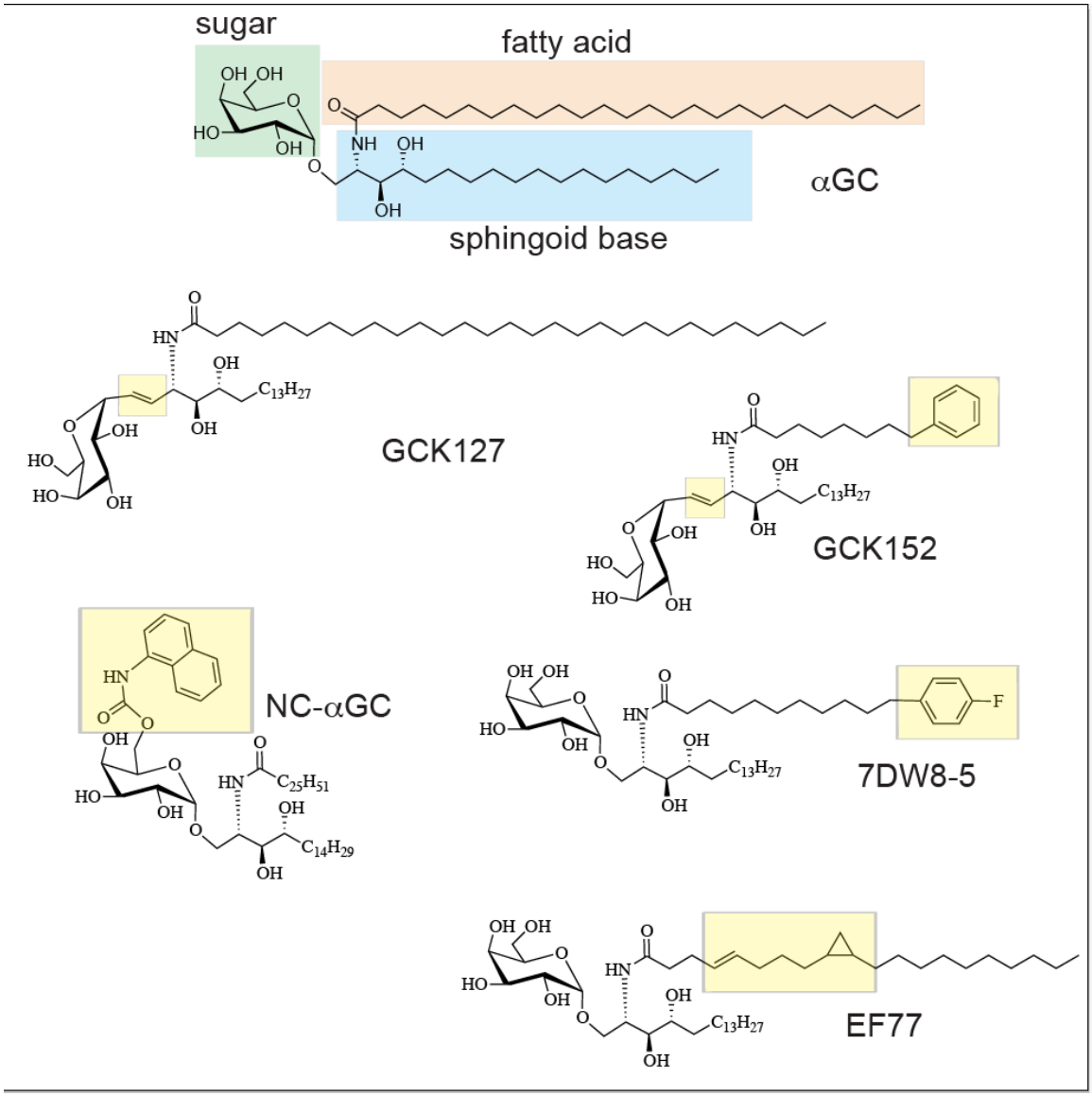

Figure 2

A. Mouse CD1d and Mouse TCR SPR Analysis			
Glycolipid	**$K_{ass}(M^{-1}S^{-1})$**	**$K_{diss}(S^{-1})$**	**$K_D(K_{diss}/K_{ass})$**
NC-αGC	3.8E+04 ± 5.30E+03	1.50E-03 ± 7.35E-04	37.1 ± 14.10 nM
EF77	4.5E+04 ± 0.6E+03	2.00E-03 ± 0.1E-03	44.7 ± 0.4 nM
7DW8-5	9.4E+04 ± 3.4E+03	8.86E-03 ± 9.31E-05	94 ± 2.8 nM
GCK152	8.5E+04 ± 1.5E+03	1.66E-02 ± 1.60E-03	197 ± 22 nM
GCK127	5.7E+04 ± 1.4E+04	1.28E-02 ± 1.4E-03	247 ± 86 nM
B. Human CD1d and Human TCR SPR Analysis			
Glycolipid	**$K_{ass}(M^{-1}S^{-1})$**	**$K_{diss}(S^{-1})$**	**$K_D(K_{diss}/K_{ass})$**
7DW8-5	10.3E+04 ± 4.7E+04	0.163 ± 0.139	1.13 ± 0.9 uM
GCK127	4.4E+04 ± 2.9E+04	0.066 ± 0.045	1.45 ± 0.05 uM
NC-αGC	14E+04 ± 2E+04	0.205 ± 0.075	1.45 ± 0.35 uM
EF77	26.25E+04 ± 17.75E+04	0.295 ± 0.005	3.4 ± 2.71 uM
GCK152	1.4E+04 ± 0.4E+04	0.107 ± 0.063	6.85 ± 2.6 uM

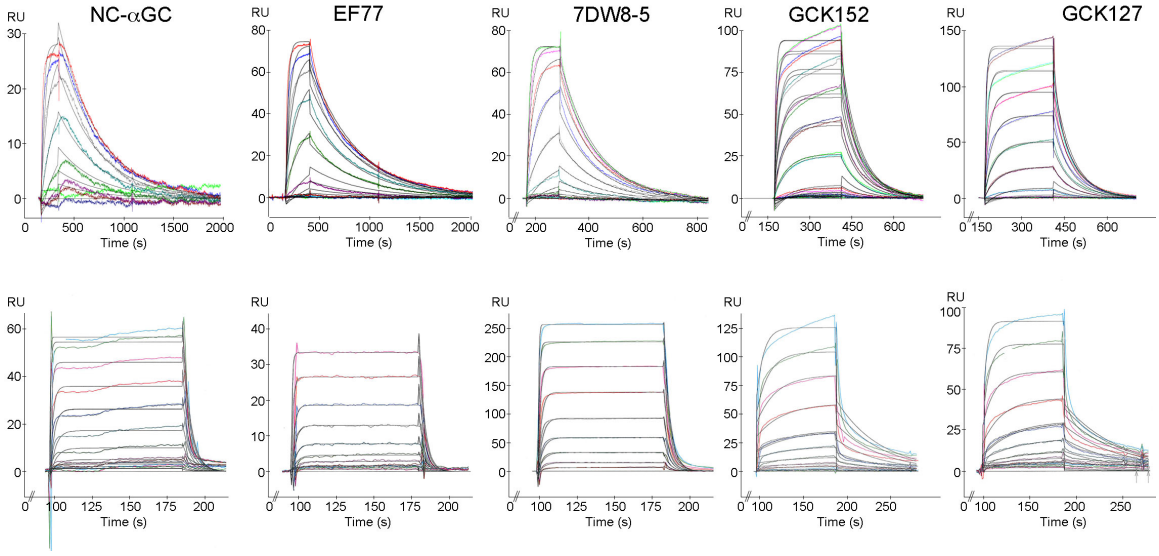

Figure 3

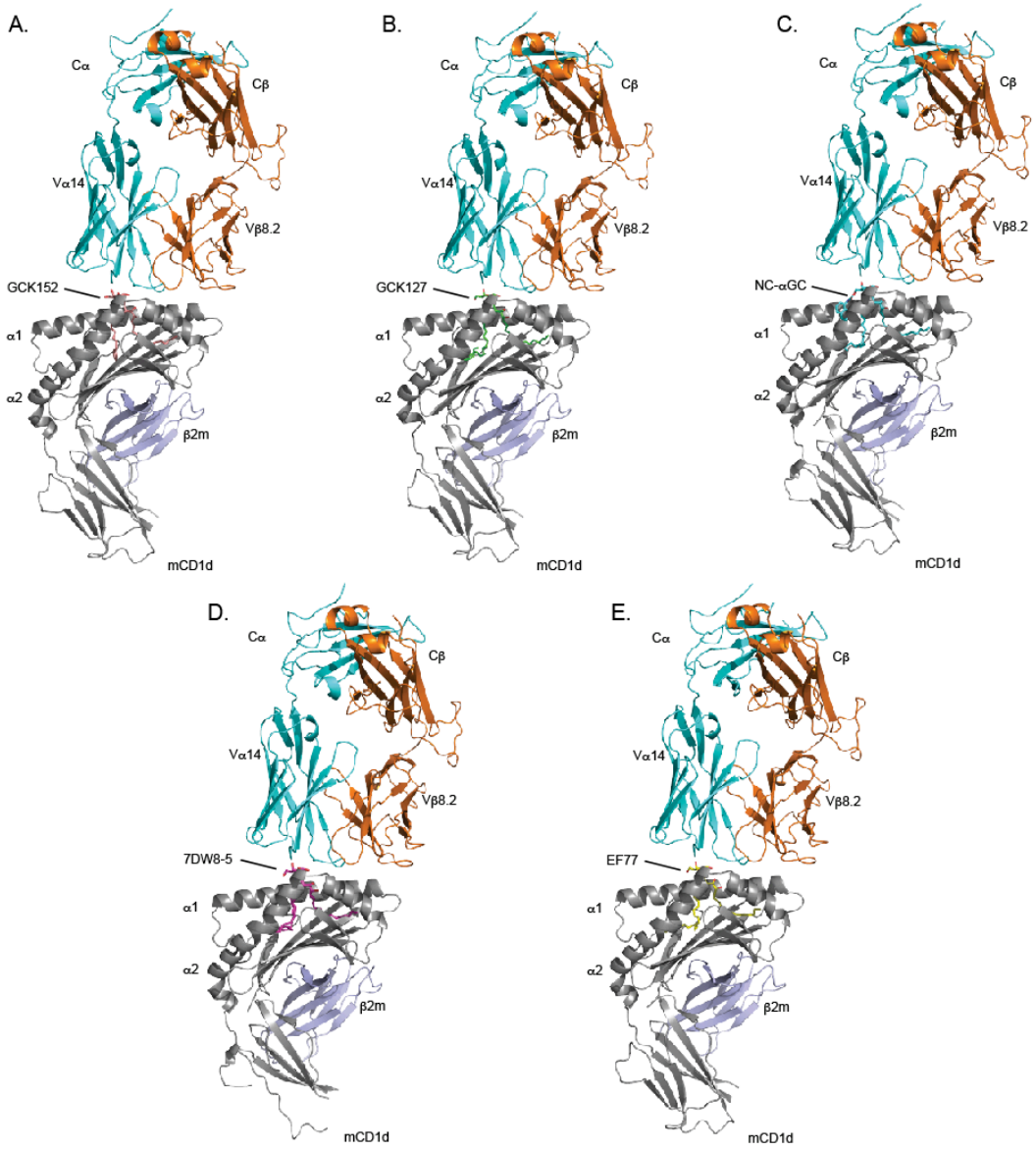
A.
Cα
Cβ
Vα14
Vβ8.2
GCK152
α1
α2
β2m
mCD1d
B.
Cα
Cβ
Vα14
Vβ8.2
GCK127
α1
α2
β2m
mCD1d
C.
Cα
Cβ
Vα14
Vβ8.2
NC-αGC
α1
α2
β2m
mCD1d
D.
Cα
Cβ
Vα14
Vβ8.2
7DW8-5
α1
α2
β2m
mCD1d
E.
Cα
Cβ
Vα14
Vβ8.2
EF77
α1
α2
β2m
mCD1d

Figure 4

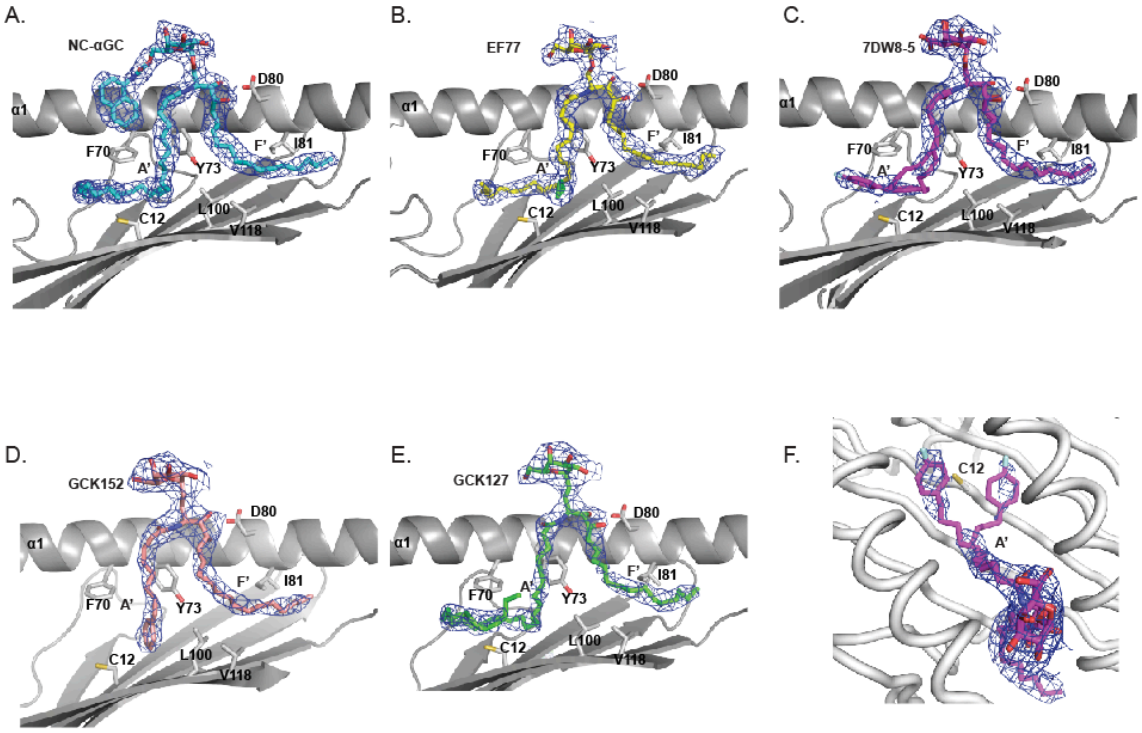
A.
NC-αGC
D80
α1
F70
A'
Y73
F'
I81
C12
L100'
V118'
B.
EF77
D80
α1
F70
A'
Y73
F'
I81
C12
L100
V118
C.
7DW8-5
D80
α1
F70
A'
Y73
F'
I81
C12
L100
V118
D.
GCK152
D80
α1
F70
A'
Y73
F'
I81
C12
L100
V118
E.
GCK127
D80
α1
F70
A'
Y73
F'
I81
C12
L100
V118
F.
C12
A'

Figure 5

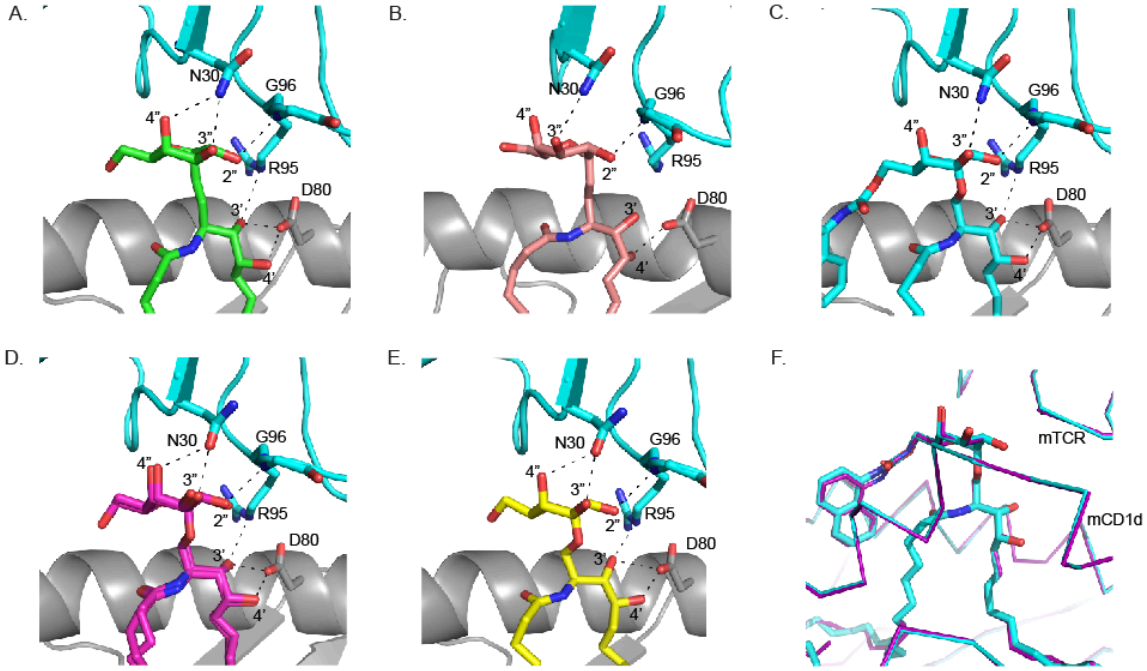

Figure 6

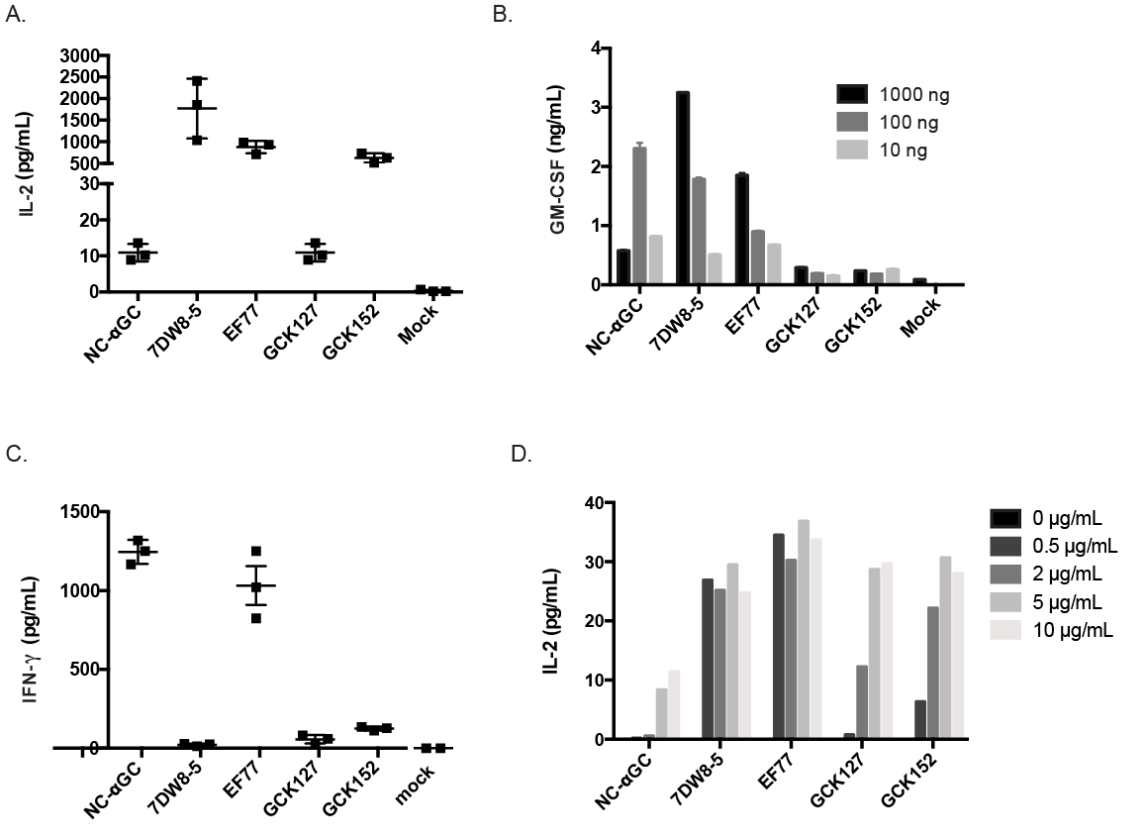
A.
IL-2 (pg/mL)
3000
2500
2000
1500
1000
500
30
20
10
0
NC-αGC
7DW8-5
EF77
GCK127
GCK152
Mock
B.
GM-CSF (ng/mL)
4
3
2
1
0
1000 ng
100 ng
10 ng
NC-αGC
7DW8-5
EF77
GCK127
GCK152
Mock
C.
IFN-γ (pg/mL)
1500
1000
500
0
NC-αGC
7DW8-5
EF77
GCK127
GCK152
mock
D.
IL-2 (pg/mL)
40
30
20
10
0
0 μg/mL
0.5 μg/mL
2 μg/mL
5 μg/mL
10 μg/mL
NC-αGC
7DW8-5
EF77
GCK127
GCK152